

## COULOMB BLOCKADE AND KONDO EFFECT IN QUANTUM DOTS

L.I. GLAZMAN<sup>1</sup> and M. PUSTILNIK<sup>2</sup>

<sup>1</sup>*Theoretical Physics Institute, University of Minnesota,  
Minneapolis, MN 55455*

<sup>2</sup>*School of Physics, Georgia Institute of Technology,  
Atlanta, GA 30332*

**Abstract.** We review the mechanisms of low-temperature electron transport across a quantum dot weakly coupled to two conducting leads. Conduction in this case is controlled by the interaction between electrons. At temperatures moderately lower than the single-electron charging energy of the dot, the linear conductance is suppressed by the Coulomb blockade. Upon further lowering of the temperature, however, the conductance may start to increase again due to the Kondo effect. This increase occurs only if the dot has a non-zero spin  $S$ . We concentrate on the simplest case of  $S = 1/2$ , and discuss the conductance across the dot in a broad temperature range, which includes the Kondo temperature. Temperature dependence of the linear conductance in the Kondo regime is discussed in detail. We also consider a simple (but realistic) limit in which the differential conductance at a finite bias can be fully investigated.

### 1. Introduction

In this review, we define a quantum dot as a small paddle of electron liquid which is attached by tunnel junctions to two massive conductors (leads). The number of electrons on the dot in equilibrium  $N$  can be controlled by varying the voltage applied to a gate – an auxiliary electrode coupled to the dot only capacitively (no tunneling occurs between the dot and gate). If the conductances of the lead-dot junctions are small compared to the conductance quantum  $e^2/h$ , and if the temperature  $T$  is low enough, then  $N$  is an integer at almost any gate voltage  $V_g$ . Exceptions are small intervals around the discrete set of values of  $V_g$ , at which an addition of a single electron to the dot does not change the electrostatic energy. Such a degeneracy between different charge states of a quantum dot allows for an activationless electron transfer through it, whereas for all other values of  $V_g$  the activation energy for the conductance  $G$  across the dot is finite. The resulting oscillatory dependence  $G(V_g)$  is the hallmark of the Coulomb blockade phenomenon [1]. The contrast between the low- and high-conductance regions (Coulomb blockade valleys and peaks, respectively) gets sharper at lower temperatures. The described pattern of the  $G(V_g, T)$  dependence is clearly observed

down to the lowest attainable temperatures in experiments on tunneling through small metallic islands [2] However, small quantum dots formed in GaAs heterostructures display a different behavior [3]: in some Coulomb blockade valleys the dependence  $G(T)$  is not monotonic and has a minimum at a finite temperature. This minimum is similar in origin [4] to the well-known non-monotonic temperature dependence of the resistivity of a metal containing magnetic impurities [5] – the Kondo effect.

We present here an introduction to the theory of Kondo effect in quantum dots, concentrating on the so-called *Constant Interaction Model*. Despite its simplicity, the model allows one to describe the main conduction mechanisms, including the most important version of the Kondo effect in quantum dots.

## 2. Constant Interaction Model

The Hamiltonian of interacting electrons confined to a quantum dot has the following general form:

$$\hat{H}_{dot} = \sum_{ij;s} \mathcal{H}_{ij} d_{is}^\dagger d_{js} + \frac{1}{2} \sum_{ss'} \sum_{ijkl} \mathcal{H}_{ijkl} d_{is}^\dagger d_{js'}^\dagger d_{ks'} d_{ls}. \quad (1)$$

Here an operator  $d_{is}^\dagger$  creates an electron with spin  $s$  in the orbital state  $\phi_i(\mathbf{r})$ ;  $\mathcal{H}_{ij} = \mathcal{H}_{ji}^*$  is an Hermitian matrix describing the single-particle spectrum, and the matrix elements  $\mathcal{H}_{ijkl}$  depend on the electron-electron interaction potential  $V(\mathbf{r}_1 - \mathbf{r}_2)$  and on the chosen basis of orbital states:

$$\mathcal{H}_{ijkl} = \int d\mathbf{r}_1 d\mathbf{r}_2 V(\mathbf{r}_1 - \mathbf{r}_2) \phi_i(\mathbf{r}_1) \phi_j(\mathbf{r}_2) \phi_k^*(\mathbf{r}_2) \phi_l^*(\mathbf{r}_1). \quad (2)$$

Further simplification of the Hamiltonian (1) is possible if the following conditions are met:

- (i) the electron-electron interaction within the dot is not too strong (the gas parameter characterizing the electron-electron interaction in a non-ideal Fermi gas  $r_s \lesssim 1$ ) so that the Fermi liquid description is applicable;
- (ii) the quasiparticle spectrum is not degenerate near the Fermi energy (which is satisfied, in general, if the motion of electrons within the dot is chaotic);
- (iii) the dot is in the metallic regime, *i.e.* the Thouless energy of the dot  $E_T$  exceeds the mean single-particle level spacing  $\delta E$ .

The Thouless energy  $E_T$  is well-defined if the electron motion within it is chaotic due to either disorder or irregular shape of the dot. For a dot of linear size  $L$  it equals

$$E_T \simeq \begin{cases} \hbar D/L^2, & l \ll L \\ \hbar v_F/L, & l \gg L \end{cases}, \quad (3)$$

where  $l$  is the elastic mean free path and  $D$  is the diffusion constant in a disordered dot. The average level spacing  $\delta E$  can be estimated as

$$\delta E \simeq 1/\nu_d L^d. \quad (4)$$

Here  $d$  is the dimensionality of the system ( $d = 2$  for a quantum dot formed in a two-dimensional electron gas in a semiconductor heterostructure, and  $d = 3$  for a metallic nanoparticle);  $\nu_d$  is the density of states of the material. For a ballistic electron motion ( $l \gg L$ ) the ratio

$$E_T/\delta E \sim L/\lambda_F \sim N^{1/d}$$

is large for large number of electrons  $N$  on the dot.

If the conditions (i)-(iii) are met, then the Random Matrix Theory (RMT) is a good starting point for describing non-interacting quasiparticles, see [6] for a review; the matrix elements  $\mathcal{H}_{ij}$  belong to a Gaussian ensemble [7]. The matrix elements do not depend on spin, and therefore each eigenvalue  $\epsilon_n$  of the matrix  $\mathcal{H}_{ij}$  represents a spin-degenerate energy level. The spacings  $|\epsilon_{n+1} - \epsilon_n|$  between consecutive levels obey the Wigner-Dyson distribution [7]; the average value of  $|\epsilon_{n+1} - \epsilon_n|$  is  $\delta E$ .

It turns out [8] that the vast majority of the matrix elements  $\mathcal{H}_{ijkl}$  are small. In the limit  $E_T/\delta E \rightarrow \infty$ , only relatively few ‘‘most diagonal’’ elements remain finite. In this limit the interaction part  $H_{int}$  of the Hamiltonian of a non-superconducting dot may be cast in the form [9]:

$$\hat{H}_{int} = E_C (\hat{N} - \mathcal{N})^2 - E_S \hat{\mathbf{S}}^2. \quad (5)$$

Here

$$\hat{N} = \sum_{ns} d_{ns}^\dagger d_{ns}, \quad \hat{\mathbf{S}} = \sum_{nss'} d_{ns}^\dagger \frac{\boldsymbol{\sigma}_{ss'}}{2} d_{ns'} \quad (6)$$

are the operators of total number of electrons and total spin on the dot. Obviously, the Hamiltonian (5) is invariant with respect to a change of the single-particle basis  $\phi_i(\mathbf{r})$ .

The first term in Eq. (5) represents the electrostatic energy. In the conventional equivalent circuit picture, see Fig. 1, the charging energy  $E_C$  is related to the total capacitance  $C$  of the dot,  $E_C = e^2/2C$ , and the dimensionless parameter  $\mathcal{N}$  is proportional to the gate voltage,  $\mathcal{N} = C_g V_g/e$ , where  $C_g$  is the capacitance between the dot and the gate. For a mesoscopic ( $\lambda_F \ll L$ ) conductor, the charging energy is large compared to the level spacing  $\delta E$ . Indeed, using the estimate  $C \sim \kappa L$ , where  $\kappa$  is the dielectric constant, we find

$$\frac{E_C}{\delta E} \sim \frac{e^2}{\kappa \hbar v_F} \left( \frac{L}{\lambda_F} \right)^{d-1} \sim r_s N^{d-1}, \quad (7)$$

where  $v_F$  is the Fermi velocity, and  $r_s$  is the conventional gas parameter. Except an exotic case of an extremely weak interaction, having a large number of electrons  $N \sim (L/\lambda_F)^d \gg 1$  on a quantum dot guarantees that the inequality  $E_C \gg \delta E$  is satisfied in dimensions  $d = 2, 3$ . For the smallest quantum dots formed in GaAs heterostructures,  $E_C/\delta E \sim 10$  [3]; for a metallic nanoparticle with  $L \simeq 5$  nm this ratio is about 100, see, e.g., [10]. We should mention also that in the  $d = 1$  case, the estimate (7) is of little help, as even a weak electron-electron interaction results in a formation of a Luttinger liquid [11], significantly affecting the nomenclature of the elementary excitations. In the case of a single-mode finite-length Luttinger liquid, the elementary excitations can be viewed as  $1d$  plasmon waves in a confined geometry, so the corresponding level spacing is  $\delta E \sim E_C$ .

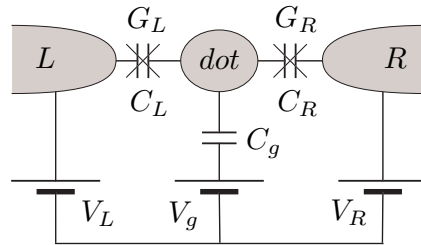


Figure 1. Equivalent circuit of a dot connected to two leads by tunnel junctions (with conductances  $G_L$  and  $G_R$ ) and coupled via a capacitor (with capacitance  $C_g$ ) to the gate. The total capacitance of the dot  $C = C_L + C_R + C_g$ .

The second term in Eq. (5) is the exchange interaction characterized by the exchange constant  $E_S$ . This constant is small in the case of weak electron-electron interaction:  $E_S \sim r_s \delta E$  (there is an additional  $\ln(1/r_s)$  factor in this estimate in the case of a  $2d$  dot). Smallness of the ratio  $E_S/\delta E$  guarantees the absence of a macroscopic (proportional to the volume of the dot) spin in the ground state, in accordance with the well-known Stoner criterion for the itinerant magnetism [12]. If all the orbital levels were equidistant, then the spin of an even-electron state would be zero, while an odd-electron state would have spin  $1/2$ . However, the level spacings  $|\epsilon_{n+1} - \epsilon_n|$  are random. If the spacing between some orbital levels is accidentally small, the dot may acquire a spin [13] exceeding  $1/2$ . At small  $r_s$ , however, such states are rare, and in the following we disregard this possibility. This allows us to neglect the exchange term in the interaction Hamiltonian (5).

Keeping in mind that Eq. (5) is invariant with respect to the rotations of the basis of single-particle states, we can pick up the basis in which the first term in the Hamiltonian (1) is diagonal. Eq. (5) then reduces to the Hamiltonian of the Constant Interaction Model,

$$\hat{H}_{dot} = \sum_{ns} \epsilon_n d_{ns}^\dagger d_{ns} + E_C (\hat{N} - \mathcal{N})^2, \quad (8)$$

which is widely used in the analysis of the experimental data. We stress that the single-particle level spacings  $|\epsilon_{n+1} - \epsilon_n| \sim \delta E$  here are small compared to the charging energy, and each single-particle state is spin-degenerate.

Electron transport through the dot occurs via two dot-lead junctions, see Fig. 1. As long as the conductances  $G_L$  and  $G_R$  of the left ( $L$ ) and right ( $R$ ) junctions are small compared to  $e^2/h$ , one may use the tunneling Hamiltonian to describe the junctions:

$$\hat{H}_t = \sum_{\alpha kn s} t_{\alpha kn} c_{\alpha ks}^\dagger d_{ns} + \text{H.c.}, \quad \alpha = R, L. \quad (9)$$

Here  $c_{\alpha ks}^\dagger$  are the creation operators of electrons in the leads, and  $t_{\alpha kn}$  are the tunneling matrix elements (tunneling amplitudes) connecting the state  $n$  in the dot with the state  $k$  in the lead  $\alpha$ . Usually it is adequate to consider the leads as reservoirs of free electrons:

$$\mathcal{H}_\alpha = \sum_{ks} \xi_{\alpha k} c_{\alpha ks}^\dagger c_{\alpha ks} \quad (10)$$

with continuous spectra  $\xi_{\alpha k}$ . In the following we will characterize these spectra by the density of states  $\nu$ , same for both leads.

The randomness of states  $n$  translates into the randomness of the tunneling amplitudes  $t_{\alpha kn}$ . Similar to the single-particle spectrum of the dot, the tunneling amplitudes can be studied in the RMT framework. Regardless the details of the statistical properties of  $t_{\alpha kn}$ , the corresponding tunneling probabilities can be related to the average conductances  $G_\alpha$  of the junctions:

$$\overline{|t_{\alpha kn}^2|} = \frac{\hbar G_\alpha}{4\pi e^2 \nu} \delta E. \quad (11)$$

The tunneling amplitudes determine also the rate  $\Gamma_\alpha$  for an electron occupying a given discrete level in the dot to escape into the lead  $\alpha = L, R$ . The escape rates are determined by the tunneling amplitudes. With the help of Eq. (11) the average values of the rates are estimated to be  $\Gamma_\alpha \sim (\hbar G_\alpha / e^2) \delta E$ .

### 3. Rate equations and conductance across the dot

At high temperatures,  $T \gg E_C$ , charging energy is negligible compared to the thermal energy of electrons. Therefore the conductance  $G_\infty$  in this regime is not affected by charging and, independently of the gate voltage,

$$\frac{1}{G_\infty} = \frac{1}{G_L} + \frac{1}{G_R}. \quad (12)$$

At lower temperatures,

$$\delta E \ll T \ll E_C, \quad (13)$$

electron transport across the dot starts to depend on  $\mathcal{N}$ . The conductance is not suppressed only within narrow regions – Coulomb blockade peaks, *i.e.*, at the gate voltages tuned sufficiently close to the points of charge degeneracy,

$$|\mathcal{N} - \mathcal{N}^*| \lesssim T/E_C; \quad (14)$$

here  $\mathcal{N}^*$  is a half-integer number.

We will demonstrate this now using the method of rate equations. In addition to the constraint Eq. (13), we will assume that the inelastic electron relaxation rate  $1/\tau_\varepsilon$  within the dot is large compared to the escape rates  $\Gamma_\alpha$ . In other words, electron transitions between discrete levels in the dot occur before the electron escapes to the leads<sup>1</sup>. Under this assumption the tunnelings across the two junctions can be treated independently of each other. The condition (14), on the other hand, allows us to take into account only two charge states of the dot which are almost degenerate in the vicinity of a Coulomb blockade peak. For  $\mathcal{N}$  close to  $\mathcal{N}^*$  these are the states with  $N = \mathcal{N}^* \pm 1/2$  electrons on the dot. Hereafter we denote these states as  $|N\rangle$  and  $|N+1\rangle$ . Finally, the condition (13) enables us to replace the discrete single-particle levels within the dot by a continuum with the density of states  $1/\delta E$ .

Applying the Fermi Golden Rule and using the described simplifications we may write the current  $I_\alpha$  from the lead  $\alpha$  into the dot as

$$I_\alpha = \frac{2\pi}{\hbar} \sum_{kns} |t_{\alpha kn}|^2 \delta(\xi_k + eV_\alpha + E_N - \epsilon_n - E_{N+1}) \\ \times \{P_N f(\xi_k)[1 - f(\epsilon_n)] - P_{N+1} f(\epsilon_n)[1 - f(\xi_k)]\}.$$

Here  $f(\omega) = [\exp(\omega/T) + 1]^{-1}$  is the Fermi function,  $V_\alpha$  is the potential on the lead  $\alpha$ , see Fig. 1,  $E_N$  and  $E_{N+1}$  are the electrostatic energies of the charge states  $|N\rangle$  and  $|N+1\rangle$ , and  $P_N$  and  $P_{N+1}$  are the probabilities to find the dot in these states. Replacing the summations over  $n$  and  $k$  by integrations over the corresponding continua, we find

$$I_\alpha = \frac{G_L}{e} [P_N F(E_1 - E_0 - \mu_\alpha) - P_{N+1} F(E_0 - E_1 + \mu_\alpha)] \quad (15)$$

with  $F(\omega) = \omega/[\exp(\omega/T) - 1]$ . In equilibrium, the current Eq. (15) is zero by the detailed balance. When a finite current flows through the junction the probabilities  $P_N$  and  $P_{N+1}$  deviate from their equilibrium values. In the steady state, the currents across the two junctions satisfy

$$I = I_L = -I_R. \quad (16)$$

---

<sup>1</sup> Note that a finite inelastic relaxation rate requires inclusion of mechanisms beyond the Constant Interaction Model, *e.g.*, electron-phonon collisions.

From Eqs. (15) and (16), supplemented by the obvious normalization condition  $P_N + P_{N+1} = 1$ , one finds the current across the dot  $I$  in response to the applied bias  $V = V_L - V_R$ . The linear conductance across the dot  $G = \lim_{V \rightarrow 0} dI/dV$  is then given by

$$G = G_\infty \frac{E_C(\mathcal{N} - \mathcal{N}^*)/T}{\sinh[2E_C(\mathcal{N} - \mathcal{N}^*)/T]}. \quad (17)$$

Here a half-integer  $\mathcal{N} = \mathcal{N}^*$  corresponds to the Coulomb blockade peak. In the Coulomb blockade valleys ( $\mathcal{N} \neq \mathcal{N}^*$ ), conductance falls off exponentially with the decreasing temperature, and all the valleys behave exactly the same way.

According to Eq. (17), all the Coulomb blockade peaks have the same height  $G(\mathcal{N}^*) = G_\infty/2$  and are symmetric about  $\mathcal{N} = \mathcal{N}^*$ . Such equivalence of all the peaks occurs because for  $T \gg \delta E$ , see Eq. (13), many energy levels in the dot make a significant contribution to the conductance. Decrease of temperature below  $\delta E$  brings about a modification of Eq. (17) in the vicinity of the Coulomb blockade peaks  $|\mathcal{N} - \mathcal{N}^*| \ll \delta E/E_C$ . In this regime the main contribution to the conductance comes from tunneling through a single energy level in the dot. The dependence  $G(\mathcal{N}, T)$  can again be found from the proper rate equations with the result [9]

$$G \propto -G_\infty \frac{\delta E}{T} \frac{df(X)/dX}{1 + f(X)}, \quad X = \frac{2E_C}{T}(\mathcal{N} - \mathcal{N}^*). \quad (18)$$

In writing Eq. (18) we neglected mesoscopic fluctuations of the peaks heights [14]. Note that according to Eq. (18) the shape of the peak is asymmetric. The asymmetry comes about from the difference in the spin states of the dots in two adjacent Coulomb blockade valleys: Eq. (18) is written for a peak separating the valley with  $N = \mathcal{N}^* - 1/2 =$  odd number of electrons at  $X < 0$  from the valley with  $N = \mathcal{N}^* + 1/2 =$  even at  $X > 0$ . The validity of Eq. (18) is restricted to the vicinity of the Coulomb blockade peak,  $|\mathcal{N} - \mathcal{N}^*| \ll \delta E/E_C$ , and for temperatures in the interval  $\Gamma_\alpha \ll T \ll \delta E$ . When the temperature falls below the escape rates  $\Gamma_\alpha$  the Coulomb blockade peaks are no longer well-defined due to the onset of the Kondo effect.

#### 4. Activationless transport through a blockaded quantum dot

According to the rate equations theory [15], at low temperatures,  $T \ll E_C$ , conduction through the dot in the Coulomb blockade valleys is exponentially suppressed. This suppression occurs because the process of electron transport through the dot involves a *real transition* to the state in which the charge of the dot differs by  $e$  from the thermodynamically most probable value. The probability of such fluctuation is proportional to  $\exp[-E_C|\mathcal{N} - \mathcal{N}^*|/T]$ , which explains the conductance suppression, see Eq. (17). Going beyond the lowest-order perturbation theory in conductances  $G_\alpha$  allows one to consider processes in which states of the

dot with a “wrong” charge participate in the tunneling process as *virtual states*. The existence of these higher-order contributions to the tunneling conductance was first envisioned by Giaever and Zeller [16]. The first quantitative theory of this effect, however, was developed much later [17].

The leading contributions to the activationless transport, according to Refs. [17], are provided by the processes of inelastic and elastic *co-tunneling*. Unlike the sequential tunneling, in the co-tunneling mechanism, the events of electron tunneling from one of the leads into the dot, and tunneling from the dot to the other lead occur as a single quantum process.

#### 4.1. INELASTIC CO-TUNNELING

In the inelastic co-tunneling mechanism, an electron tunnels from the lead into one of the vacant single-particle levels in the dot, while it is an electron occupying some other level that tunnels out of the dot, see Fig. 2(a). As a result, transfer of charge  $e$  between the leads is accompanied by a simultaneous creation of an electron-hole pair in the dot.

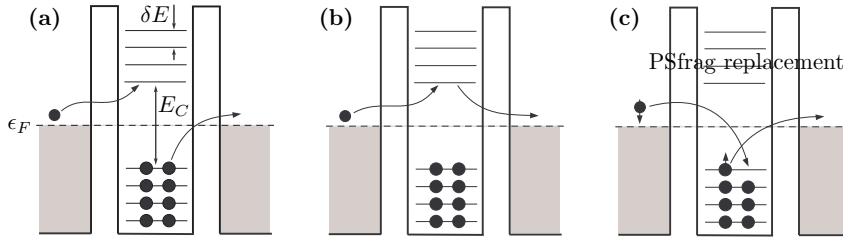


Figure 2. Examples of the co-tunneling processes.

(a) inelastic co-tunneling: transferring of an electron between the leads leaves behind an electron-hole pair in the dot; (b) elastic co-tunneling; (c) elastic co-tunneling with a flip of spin.

Here we will estimate the contribution of the inelastic co-tunneling to the conductance deep in the Coulomb blockade valley, *i.e.*, at almost integer  $\mathcal{N}$ . Consider an electron that tunnels into the dot from the lead  $\alpha$ . If the energy of the electron relative to the Fermi level  $\omega$  is small compared to the charging energy,  $\omega \ll E_C$ , then the energy of the virtual state involved in the co-tunneling process is close to  $E_C$ . The amplitude  $A_{in}$  of the inelastic transition via this virtual state is then given by

$$\mathcal{A}_{\alpha \rightarrow \alpha'}^{in} = \frac{t_{\alpha k n}^* t_{\alpha' k' n'}}{E_C}. \quad (19)$$

The initial state of this transition has an extra electron in the single-particle state  $k$  in the lead  $\alpha$ , while the final state has an extra electron in the state  $k'$  in the lead  $\alpha'$  and an electron-hole pair in the dot (state  $n$  is occupied, state  $n'$  is empty).

Given the energy of the initial state  $\omega$ , the number of available final states can be estimated from the phase space argument, familiar from the calculation of the quasiparticle lifetime in the Fermi liquid theory [18]. For  $\omega \gg \delta E$  this number is of the order of  $(\omega/\delta E)^2$ . Since the typical value of  $\omega$  is  $T$ , the inelastic co-tunneling contribution to the conductance can be estimated as

$$G_{in} \sim \frac{e^2}{h} \left( \frac{T}{\delta E} \right)^2 \nu^2 |\mathcal{A}_{L \rightarrow R}^{in}|^2.$$

Using Eqs. (19) and (11) we find [17]

$$G_{in} \sim \frac{h}{e^2} G_L G_R \left( \frac{T}{E_C} \right)^2. \quad (20)$$

A comparison of Eq. (20) with the result of the rate equations theory Eq. (17) shows that the inelastic co-tunneling takes over the thermally-activated hopping at moderately low temperatures

$$T \lesssim T_{in} = E_C \left[ \ln \left( \frac{e^2/h}{G_L + G_R} \right) \right]^{-1}. \quad (21)$$

The smallest energy of the electron-hole pair is of the order of  $\delta E$ . At temperatures below this threshold the inelastic co-tunneling contribution to the conductance becomes exponentially small. It turns out, however, that even at much higher temperatures this mechanism becomes less effective than the elastic co-tunneling.

#### 4.2. ELASTIC CO-TUNNELING

In the process of elastic co-tunneling, transfer of charge between the leads is not accompanied by the creation of an electron-hole pair in the dot. In other words, occupation numbers of single-particle energy levels in the dot in the initial and final states of the co-tunneling process are exactly the same, see Fig. 2(b). Here we will estimate the elastic co-tunneling contribution to the conductance near the edge of a Coulomb-blockade valley,

$$\delta E/E_C \ll \mathcal{N} - \mathcal{N}^* \ll 1/2. \quad (22)$$

Under this condition, the average number of electrons on the dot  $N = \mathcal{N}^* + 1/2$ . A cost in electrostatic energy for a removal of a single electron from the dot,  $E_- = 2E_C(\mathcal{N} - \mathcal{N}^*)$ , see Eq. (8), is small compared to the cost to add an electron  $E_+ \approx 2E_C$  [here we took into account the second inequality in Eq. (22)]. Therefore, only hole-like virtual states with  $N - 1$  electrons on the dot contribute to the co-tunneling amplitude:

$$\mathcal{A}_{\alpha \rightarrow \alpha'}^{el} = \sum_{\epsilon_n \leq 0} A_{\alpha \rightarrow \alpha'}^n, \quad A_{\alpha \rightarrow \alpha'}^n = \frac{t_{\alpha k n}^* t_{\alpha' k' n}}{E_- + |\epsilon_n|}. \quad (23)$$

Here  $A^n$  represent amplitudes of the processes in which a hole is virtually created on  $n$ th single-particle level. Creation of a hole is only possible if the level is occupied, hence the restriction of the sum in Eq. (23) to the levels below the Fermi level ( $\epsilon_n \leq 0$ ).

The elastic co-tunneling contribution to the conductance is

$$G_{el} = \frac{e^2}{\pi\hbar} \nu^2 \left| \mathcal{A}_{L \rightarrow R}^{el} \right|^2. \quad (24)$$

If the dot-leads junctions are point contacts, then  $G_{el}$  exhibits strong mesoscopic fluctuations. Indeed, tunneling matrix elements entering Eq. (23) depend on the values of the electron wave functions at the points  $\mathbf{r}_\alpha$  of the contacts,  $t_{\alpha kn} \propto \varphi_n(\mathbf{r}_\alpha)$ . In the RMT model, briefly discussed in Section 2, the electron wave functions in the dot  $\varphi_n(\mathbf{r})$  are random and uncorrelated,  $\overline{\varphi_n(\mathbf{r}_\alpha) \varphi_{n'}(\mathbf{r}_{\alpha'})} \propto \delta_{nn'} \delta_{\alpha\alpha'}$ . Therefore, the partial amplitudes  $A_{L \rightarrow R}^n$  are random and uncorrelated as well:

$$\overline{(A_{L \rightarrow R}^n)^* A_{L \rightarrow R}^m} = \delta_{nm} \overline{|A_{L \rightarrow R}^n|^2}.$$

Eqs. (23),(24) and (11) then yield for the average conductance

$$\overline{G_{el}} = \frac{e^2}{\pi\hbar} \nu^2 \sum_{\epsilon_n \leq 0} \overline{|A_{L \rightarrow R}^n|^2} \sim \frac{h}{e^2} G_L G_R \sum_{\epsilon_n \leq 0} \left[ \frac{\delta E}{E_- + |\epsilon_n|} \right]^2.$$

Since under the conditions (22) the number of terms making significant contribution to the sum over  $n$  here is large, and since the sum is converging, one can replace the summation by an integral which results in [17]

$$\overline{G_{el}} \sim \frac{h}{e^2} G_L G_R \frac{\delta E}{E_C} \left[ \frac{1}{\mathcal{N} - \mathcal{N}^*} + \frac{1}{\mathcal{N}^* - \mathcal{N} + 1} \right]. \quad (25)$$

Here we have included both the hole-like and electron-like contributions to the conductance and restored the explicit dependence on the gate voltage  $\mathcal{N}$ ; Eq. (25) is valid for  $|\mathcal{N} - \mathcal{N}^* - 1/2| \ll 1/2 - \delta E/E_C$ . Comparison of Eq. (25) with Eq. (20) shows that the elastic co-tunneling dominates the electron transport already at temperatures

$$T \lesssim T_{el} = \sqrt{E_C \delta E}, \quad (26)$$

which may exceed significantly the level spacing.

Note that mesoscopic fluctuations of the elastic co-tunneling contribution to the conductance  $G_{el}$  are of the order of its average and get stronger when the gate voltage is tuned closer to the middle of the Coulomb blockade valley [19]. Thus, although  $\overline{G_{el}}$  is always positive, see Eq. (25), the sample-specific value of  $G_{el}$  for a given gate voltage may vanish.

### 5. Kondo regime in transport through a blockaded quantum dot

Among the  $E_C|\mathcal{N}-\mathcal{N}^*|/\delta E$  virtual states participating in the elastic co-tunneling through a blockaded dot, the top-most occupied single-particle level is special. If the number of electrons on the dot  $N$  is odd, this level is filled by a single electron and is spin-degenerate. Therefore the ground state of the dot is characterized not only by the occupations of the single-particle energy levels, but also by the dot's spin. This opens a possibility of a co-tunneling process in which a transfer of an electron between the leads is accompanied by a flip of electron's spin with simultaneous flip of the spin on the dot, see Fig. 2(c). The amplitude of such a process, calculated in the fourth order in tunneling matrix elements, diverges logarithmically when the energy  $\omega$  of an incoming electron approaches 0. Since  $\omega \sim T$ , the logarithmic singularity in the transmission amplitude translates into a dramatic enhancement of the conductance  $G$  across the dot at low temperatures:  $G$  may reach values as high as the quantum limit  $2e^2/h$  [20, 21]. This conductance enhancement is not really a surprise. Indeed, in the spin-flip co-tunneling process a quantum dot with odd  $N$  behaves as  $S = 1/2$  magnetic impurity embedded into a tunneling barrier separating two massive conductors. It is known [22] since mid-60's that the presence of such impurities leads to zero-bias anomalies in tunneling conductance [23], which are adequately explained [24] in the context of the Kondo effect [5].

For simplicity, we will assume here that the gate voltage  $\mathcal{N}$  is tuned to the middle of the Coulomb blockade valley with  $N = \text{odd}$  electrons on the dot. The tunneling (9) mixes this state with states having  $N \pm 1$  electrons. The electrostatic energies of these states are high ( $\sim E_C$ ), hence the transitions  $N \rightarrow N \pm 1$  are virtual, and can be taken into account perturbatively in the second order in tunneling amplitudes. The resulting effective Hamiltonian, valid at energies well below the threshold ( $\sim \delta E$ ) for spin excitations within the dot, has the form

$$H_{eff} = \sum_{\alpha ks} \xi_k c_{\alpha ks}^\dagger c_{\alpha ks} + \frac{4}{E_C} \sum_{\alpha\alpha'} \sum_{nn'} t_{\alpha n}^* t_{\alpha' n'} (\mathbf{s}_{\alpha'\alpha} \cdot \mathbf{S}_{nn'}). \quad (27)$$

Here

$$\mathbf{s}_{\alpha\alpha'} = \sum_{kk'ss'} c_{\alpha ks}^\dagger \frac{\boldsymbol{\sigma}_{ss'}}{2} c_{\alpha'k's'}, \quad \mathbf{S}_{nn'} = \mathcal{P} \left[ \sum_{ss'} d_{ns}^\dagger \frac{\boldsymbol{\sigma}_{ss'}}{2} d_{n's'} \right] \mathcal{P},$$

and  $\mathcal{P}$  is a projector onto the spin-degenerate ground state of an isolated dot. In the derivation of Eq. (27) we have replaced the tunneling amplitudes  $t_{\alpha kn}$  by their values  $t_{\alpha n}$  at the Fermi level. In addition, we have dropped the potential scattering terms associated with usual elastic co-tunneling. The latter approximation is well justified when the conductances of the dot-leads junctions are small,  $G_\alpha \ll e^2/h$ , in which case  $G_{el}$  is also very small, see Eq. (25).

By  $SU(2)$  symmetry, the operators  $\mathbf{S}_{nn'}$  for any  $n$  and  $n'$  must be proportional to  $\mathbf{S} = \mathcal{P}\hat{\mathbf{S}}\mathcal{P}$  with  $\hat{\mathbf{S}}$  being the operator of the total spin on the dot introduced in Eq. (6) above:  $\mathbf{S}_{nn'} = \lambda_{nn'}\mathbf{S}$ . Substitution into Eq. (27) then yields [25]

$$H_{eff} = \sum_{\alpha ks} \xi_k c_{\alpha ks}^\dagger c_{\alpha ks} + \sum_{\alpha\alpha'} J_{\alpha\alpha'} (\mathbf{s}_{\alpha'\alpha} \cdot \mathbf{S}) \quad (28)$$

with

$$J_{\alpha\alpha'} = \frac{4}{E_C} \sum_{nn'} t_{\alpha n}^* \lambda_{nn'} t_{\alpha' n'}. \quad (29)$$

Under the conditions of applicability of the Constant Interaction Model Eq. (8), the effective exchange Hamiltonian (28) can be simplified even further. Indeed, in this case the ground state of an isolated dot is a singlet or a doublet, depending only on the parity of  $N$ . If  $N$  is odd, then  $\mathbf{S}$  is spin-1/2 operator. The entire spin of the dot is now due to the only singly occupied single-particle energy level in it (denoted by  $n = 0$  hereafter). The matrix  $\lambda_{nn'}$  then reduces to  $\lambda_{nn'} = \delta_{nn'}\delta_{n0}$ , and Eq. (29) yields

$$J_{\alpha\alpha'} = \frac{4}{E_C} t_{\alpha 0}^* t_{\alpha' 0}. \quad (30)$$

The  $2 \times 2$  Hermitian matrix  $\hat{J}$  with elements given by Eq. (30) has an important property: since  $\det \hat{J} = 0$ , one of its eigenvalues vanishes, while the remaining eigenvalue,

$$J = \text{Tr} \hat{J} = \frac{4}{E_C} (|t_{L0}^2| + |t_{R0}^2|), \quad (31)$$

is strictly positive. By an appropriate rotation in the  $R - L$  space the Hamiltonian (28) can then be brought into the "block-diagonal" form

$$H_{eff} = H[\varphi] + H[\psi] \quad (32)$$

with

$$H[\varphi] = \sum_{ks} \xi_k \varphi_{ks}^\dagger \varphi_{ks}, \quad (33)$$

$$H[\psi] = \sum_{ks} \xi_k \psi_{ks}^\dagger \psi_{ks} + J(\mathbf{s}_\psi \cdot \mathbf{S}). \quad (34)$$

Here  $\mathbf{s}_\psi = \sum_{kk'ss'} \psi_{ks}^\dagger (\boldsymbol{\sigma}_{ss'}/2) \psi_{k's'}$ , and the operators  $\psi$  and  $\varphi$  are certain linear combinations of the original operators  $c_{R,L}$ .

To get an idea about the physics of the Kondo model, let us first replace the operator  $\mathbf{s}_\psi$  in Eq. (34) by spin-1/2 operator  $\mathbf{S}_\psi$ . The ground state of the resulting Hamiltonian of two spins  $\tilde{H} = J(\mathbf{S}_\psi \cdot \mathbf{S})$  is obviously a singlet. The excited state (a triplet) is separated from the ground state by the energy gap  $J > 0$ . This separation can be interpreted as the binding energy of the singlet. Unlike  $\mathbf{S}_\psi$  in

this simple example, the operator  $s_\psi$  in Eq. (34) is merely a spin density of the conduction electrons at the site of the "magnetic impurity". Because conduction electrons are freely moving in space, it is hard for the impurity to "capture" an electron and form a singlet. Yet, even a weak local exchange interaction suffices to form a singlet ground state [28, 29]. However, the binding energy of this singlet is given not by the exchange constant  $J$ , but by the so-called Kondo temperature

$$T_K \sim \delta E \exp(-1/\nu J). \quad (35)$$

With the help of Eqs. (31) and (11) one obtains from Eq. (35) the estimate

$$\ln\left(\frac{\delta E}{T_K}\right) \sim \frac{1}{\nu J} \sim \frac{e^2/h}{G_L + G_R} \frac{E_C}{\delta E}. \quad (36)$$

Since  $G_\alpha \ll e^2/h$ , and  $E_C \gg \delta E$ , the r.h.s. of Eq. (36) is a product of two large parameters. Therefore, the Kondo temperature  $T_K$  is small compared to the mean level spacing in the dot:

$$T_K \ll \delta E. \quad (37)$$

It is this separation of the energy scales that justifies the use of the effective low-energy Hamiltonian (27) for the description of the Kondo effect in a quantum dot system. The inequality (37) remains valid even if the conductances of the dot-leads junctions  $G_\alpha$  are of the order of  $2e^2/h$ . However, in this case neither Eq. (31) nor the estimate Eq. (36) are applicable [30].

As it follows from Eqs. (33) and (34), one of the "channels" ( $\varphi$ ) of conduction electrons completely decouples<sup>2</sup> from the dot, while the  $\psi$ -particles are described by the standard single-channel antiferromagnetic Kondo model [5]. Therefore, the thermodynamic properties of a quantum dot in the Kondo regime are identical to those of the conventional Kondo problem for a single magnetic impurity in a bulk metal; thermodynamics of the latter model is fully studied [26]. However, all the experiments addressing the Kondo effect in quantum dots test their transport properties rather than thermodynamics. The electron current operator is not diagonal in the  $(\psi, \phi)$  representation, and the contributions of these two sub-systems to the conductance are not additive. In the following we establish the relations of linear conductance and, in some special case, of the non-linear differential conductance as well, to the t-matrix of the conventional Kondo problem.

---

<sup>2</sup> It should be emphasized that the decoupling is characteristic of the Constant Interaction Model rather than a generic property. In general, both electronic channels are coupled to the dot. This, however, does not lead to qualitative changes in the results if spin of the dot is 1/2, see [25].

## 5.1. LINEAR RESPONSE

The linear conductance can be calculated from the Kubo formula

$$G = \lim_{\omega \rightarrow 0} \frac{e^2}{\hbar} \frac{1}{\omega} \int_0^\infty dt e^{i\omega t} \langle [j(t), j(0)] \rangle, \quad (38)$$

where the particle current operator  $j$  is given by

$$j = \frac{d}{dt} \frac{1}{2} (\hat{N}_R - \hat{N}_L). \quad (39)$$

Here  $\hat{N}_\alpha = \sum_{ks} c_{\alpha ks}^\dagger c_{\alpha ks}$  is the operator of the total number of electrons in the lead  $\alpha$ . In order to take the full advantage of the decomposition (32)-(34), we need to rewrite  $j$  in terms of the operators  $\psi, \varphi$ . These operators are related to the original operators  $c_{R,L}$  representing the electrons in the right and left leads via

$$\begin{pmatrix} \psi_{ks} \\ \varphi_{ks} \end{pmatrix} = \hat{U}^* \begin{pmatrix} c_{Rks} \\ c_{Lks} \end{pmatrix}, \quad (40)$$

where  $\hat{U}$  is  $2 \times 2$  unitary matrix that diagonalizes the matrix of the exchange constants (29):  $\hat{U} \hat{J} \hat{U}^\dagger = \text{diag}\{J, 0\}$ . The matrix  $\hat{U}$  can be parametrized as

$$\hat{U} = e^{i\theta_0 \tau_y} e^{i\phi_0 \tau_z}, \quad (41)$$

where  $\tau_i$  are the Pauli matrices acting in the R-L space ( $\tau_+ = \tau_x + i\tau_y$  transforms  $L$  to  $R$ ) and the angle  $\theta_0$  satisfies  $\tan \theta_0 = |t_{L0}/t_{R0}|$ . It follows from Eqs. (40) and (41) that, independently of  $\phi_0$ ,

$$\hat{N}_R - \hat{N}_L = \cos(2\theta_0) (\hat{N}_\psi - \hat{N}_\varphi) - \sin(2\theta_0) \sum_{ks} (\psi_{ks}^\dagger \varphi_{ks} + \varphi_{ks}^\dagger \psi_{ks}). \quad (42)$$

Note that the current operator  $j$  entering the Kubo formula (38) is to be calculated with the equilibrium Hamiltonian (32)-(34). Since both  $\hat{N}_\psi$  and  $\hat{N}_\varphi$  commute with  $H_{eff}$ , the first term in Eq. (42) makes no contribution to  $j$ . When the second term in (42) is substituted into Eq. (39) and then into Eq. (38), the result, after integration by parts, can be expressed via 2-particle correlation functions such as  $\langle \psi^\dagger(t) \varphi(t) \varphi^\dagger(0) \psi(0) \rangle$ . Due to the block-diagonal structure of  $H_{eff}$ , see Eq. (32), these correlation functions factorize into products of single-particle correlation functions describing the (free)  $\varphi$ -particles and the (interacting)  $\psi$ -particles. The result of the evaluation of the Kubo formula can then be written as<sup>3</sup>

$$G = G_0 \int d\omega (-df/d\omega) \frac{1}{2} \sum_s [-\pi \nu \text{Im} T_s(\omega)]. \quad (43)$$

<sup>3</sup> Further details about this calculation can be found, e.g., in the Appendix B of Ref. [27].

Here

$$G_0 = \frac{2e^2}{h} \sin^2(2\theta_0) = \frac{2e^2}{h} \left| \frac{2t_{L0}t_{R0}}{|t_{L0}^2| + |t_{R0}^2|} \right|^2, \quad (44)$$

$f(\omega)$  is the Fermi function, and  $T_s$  is the t-matrix for the Kondo model Eq. (34). The t-matrix is related to the exact retarded Green function of the  $\psi$ -particles in the usual way:

$$G_{ks,k's'}(\omega) = G_k^0(\omega) + G_k^0(\omega) [\delta_{ss'} T_s(\omega)] G_{k'}^0(\omega), \quad (45)$$

Here  $G_k^0(\omega) = (\omega - \xi_k + i0)^{-1}$  and  $G_{ks,k's'}(\omega)$  is the Fourier transform of

$$G_{ks,k's'}(t) = -i\theta(t) \left\langle \left\{ \psi_{ks}(t), \psi_{k's'}^\dagger \right\} \right\rangle,$$

where  $\langle \dots \rangle$  stands for the thermodynamic averaging with the Hamiltonian (34). In writing Eq. (45) we took into account the conservation of the total spin (which implies that  $G_{ks,k's'}$  is diagonal in  $s, s'$ ) and the fact that the interaction in Eq. (34) is local (which in turn means that the t-matrix is independent of  $k$  and  $k'$ ).

#### 5.1.1. Weak coupling regime: $T_K \ll T \ll \delta E$

Kondo effect becomes important at low temperatures  $T \sim T_K \ll \delta E$ . The exchange term in the Hamiltonian (34), however, describes transitions between the electronic states within the band of the width  $2D_0$  with  $D_0 \sim \delta E$  centered at the Fermi level  $\epsilon_F$ . The transitions between the states close to  $\epsilon_F$  and the states within a narrow strip of energies of the width  $\delta D$  near the edges of the band are associated with high energy deficit  $\sim \delta E \gg T$ . Hence, these transitions are virtual and their influence on the states near  $\epsilon_F$  can be taken into account perturbatively in the second order. This yields an effective Hamiltonian acting within the band of a reduced width  $D = D_0 - \delta D$ , which turns out to have the same form as Eq. (34), but with a modified value of the exchange amplitude  $J$  [32]. Successive reductions of the bandwidth by small steps  $\delta D$  can be viewed as a continuous process during which the initial Hamiltonian Eq. (34) is transformed to an effective low-energy Hamiltonian acting within the band of the width  $D \ll D_0$ . The evolution of the exchange amplitude during this transformation (known as the poor man's scaling [32]) can be cast into the form of an equation

$$\frac{dJ}{d\zeta} = \nu J^2, \quad \zeta = \ln(D_0/D).$$

The renormalization described by this equation can be continued until the bandwidth  $D$  becomes of the order of the temperature  $T$  or relevant electron energy  $|\omega|$ . The resulting effective exchange constant is  $\omega$ - and  $T$ -dependent [32, 33],

$$\nu J(\omega, T) = \left[ \ln \frac{\max\{|\omega|, T\}}{T_K} \right]^{-1}. \quad (46)$$

Calculation of the t-matrix in the lowest (second) order in  $\nu J(\omega, T)$  results in

$$-\pi\nu\text{Im}T_s(\omega) = \frac{3\pi^2}{16} [\nu J(\omega, T)]^2. \quad (47)$$

Substitution of (47) and (46) into Eq. (43) and evaluation of the integral over  $\omega$  with the logarithmic accuracy then yield for the conductance across the dot

$$G = G_0 \frac{3\pi^2/16}{[\ln(T/T_K)]^2}, \quad T_K \ll T \ll \delta E. \quad (48)$$

Corrections to Eq. (48) contain higher powers of  $1/\ln(T/T_K)$ . Thus, it is often said that Eq. (48) represents the conductance in the *leading logarithmic approximation*.

### 5.1.2. Strong coupling regime: $T \ll T_K$

As temperature approaches  $T_K$ , the leading logarithmic approximation result diverges, see Eq. (48). This divergence signals the failure of the approximation, as the conductance in any case can not grow higher than  $2e^2/h$ . To obtain a more precise bound, we consider in this section the conductance in the strong coupling regime  $T \ll T_K$ .

We start with the zero-temperature limit  $T = 0$ . Since, as discussed above, the ground state of the Hamiltonian (34) is not degenerate, the scattering of conduction electrons by a quantum dot is completely characterized by the scattering phase shifts  $\delta_s$  for electrons with spin  $s$  at the Fermi level. The t-matrix is then given by the standard scattering theory expression

$$-\pi\nu T_s(0) = \frac{1}{2i} (e^{2i\delta_s} - 1) = e^{i\delta_s} \sin \delta_s. \quad (49)$$

In order to find the two phase shifts  $\delta_s$ , we need two independent relations. The first one follows from the invariance of the Kondo Hamiltonian (34) under the particle-hole transformation  $\psi_{k_s} \rightarrow s\psi_{-k, -s}^\dagger$  (here  $s = \pm 1$  for spin-up/down electrons and  $k$  is counted from  $k_F$ ). The particle-hole symmetry implies the relation for the t-matrix

$$T_s(\omega) = -T_{-s}^*(-\omega),$$

valid at all  $\omega$  and  $T$ . In view of Eq. (49), it translates into the relation for the phase shifts at the Fermi level ( $\omega = 0$ ):

$$\delta_s + \delta_{-s} = 0 \pmod{\pi}. \quad (50)$$

Note that, as it is obvious from Eq. (49), the phase shifts are defined only modulo  $\pi$  (that is,  $\delta_s$  and  $\delta_s + \pi$  describe equivalent scattering states). This ambiguity can be removed by setting the values of the phase shifts corresponding to  $J = 0$  in Eq. (34) to zero. With this convention, Eq. (50) becomes

$$\delta_\uparrow + \delta_\downarrow = 0. \quad (51)$$

The second relation follows from the fact that the ground state of our system is a singlet at  $J > 0$ . In the absence of exchange ( $J = 0$ ) and at  $T = 0$ , an infinitesimally small magnetic field acting on the dot's spin,

$$\delta H[\psi] = BS^z, \quad B \rightarrow +0,$$

would polarize it. Since the free electron gas has zero spin in the ground state, the total spin in any large but finite region of space  $\mathcal{V}$  surrounding the dot coincides with the spin of the dot,  $\langle S^z \rangle_{J=0} = -1/2$ . If the exchange with electron gas is now turned on,  $J > 0$ , the infinitesimally weak field will not prevent the formation of a singlet ground state. In this state, the total spin within the region  $\mathcal{V}$  is zero. Such change of the spin is possible only if the numbers of spin-up and spin-down electrons in this region have changed in order to compensate for the spin of the dot:

$$\delta N_\uparrow - \delta N_\downarrow = 1, \quad \delta N_s = \langle \hat{N}_s \rangle_{J>0} - \langle \hat{N}_s \rangle_{J=0}. \quad (52)$$

Here  $\hat{N}_s$  are operators of the number of electrons with spin  $s$  within the region  $\mathcal{V}$ . By the Friedel sum rule,  $\delta N_s$  are related to the scattering phase shifts:  $\delta N_s = \delta_s/\pi$ . Eq. (52) then gives

$$\delta_\uparrow - \delta_\downarrow = \pi. \quad (53)$$

Combining Eqs. (51) and (53), we find  $|\delta_s| = \pi/2$ . Eqs. (43) and (49) then yield for zero-temperature conductance across the dot [20]

$$G(0) = G_0 \frac{1}{2} \sum_s \sin^2 \delta_s = G_0. \quad (54)$$

Thus, the growth of the conductance across the dot with lowering the temperature is limited only by the value of  $G_0$ . This value, see Eq. (44), depends only on the ratio of the tunneling amplitudes  $|t_{L0}/t_{R0}|$  between the leads and the last occupied single-particle energy level in the dot. If  $|t_{L0}| = |t_{R0}|$ , the conductance at  $T = 0$  will reach the maximal value  $G = 2e^2/h$  allowed by quantum mechanics [20].

The ground state of the Kondo Hamiltonian (34) is a singlet formed by the spin of the dot and a spin made up of the spins of conduction electrons. Finite-temperature correction to Eq. (55) can be found by considering virtual transitions from the singlet ground state to excited states in which the singlet is broken up [34]. The transitions can be studied by an expansion in inverse powers of the singlet binding energy  $T_K$ . The reader is referred to the original papers [34] for the details about this approach. Here we just quote the result for the imaginary part of the t-matrix [35]:

$$-\pi\nu \text{Im} T_s(\omega) = 1 - \frac{3\omega^2 + \pi^2 T^2}{2T_K^2}, \quad |\omega|, T \ll T_K \quad (55)$$

Substitution of Eq. (55) into Eq. (43) yields

$$G = G_0 \left[ 1 - (\pi T/T_K)^2 \right], \quad T \ll T_K \quad (56)$$

Accordingly, corrections to the conductance are quadratic in temperature – a typical result for the Fermi liquid theory [34].

The weak-coupling ( $T \gg T_K$ ) and the strong-coupling ( $T \ll T_K$ ) asymptotes of the conductance have a strikingly different structure. Nevertheless, since the Kondo effect is a crossover phenomenon rather than a phase transition [26, 28, 29], the dependence  $G(T)$  is a smooth and featureless [36] function throughout the crossover region  $T \sim T_K$ .

Finally, note that both Eqs. (48) and (56) have been obtained here for the particle-hole symmetric model (34). This approximation is equivalent to neglecting the elastic co-tunneling contribution to the conductance  $G_{el}$ . The asymptotes (48),(54), however, remain qualitatively correct [25] as long as  $G_{el}/G_0 \ll 1$ . The overall temperature dependence of the linear conductance in the Coulomb blockade valley in the presence of the Kondo effect is sketched in Fig. 3.

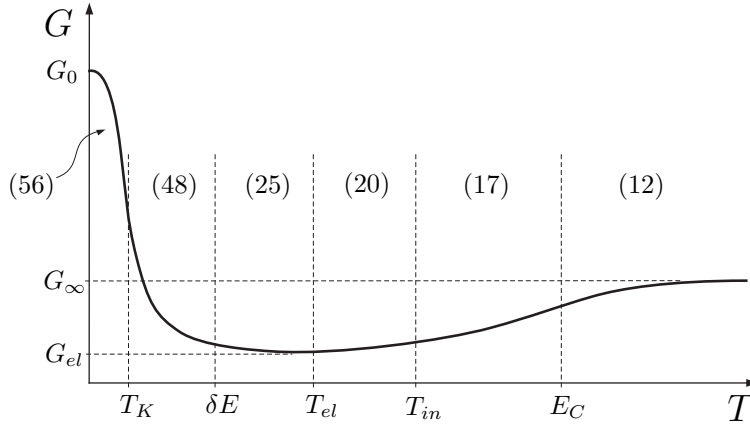


Figure 3. Schematic temperature dependence of the conductance in the middle of the Coulomb blockade valley with  $N =$  odd electrons on the dot. The numbers in brackets refer to the corresponding equations in the text.

## 5.2. BEYOND LINEAR RESPONSE

In order to study transport through a quantum dot away from equilibrium we add to the effective Hamiltonian (32)-(34) a term

$$H_V = \frac{eV}{2} (\hat{N}_L - \hat{N}_R)$$

describing a finite voltage bias  $V$  applied between the left and right electrodes. Here we will evaluate the current across the dot at arbitrary  $V$  but under the simplifying assumption that the dot-lead junctions are strongly asymmetric:  $G_L \ll G_R$ . Under this condition the angle  $\theta_0$  in Eq. (41) is small,

$$\theta_0 \approx |t_{L0}/t_{R0}| \ll 1.$$

Expanding Eq. (42) to the linear order in  $\theta_0$  we obtain

$$\begin{aligned} H_V(\theta_0) &= \frac{eV}{2} (\hat{N}_\varphi - \hat{N}_\psi) + eV\theta_0\hat{A}, \\ \hat{A} &= \sum_{ks} \varphi_{ks}^\dagger \psi_{ks} + \text{H.c.} \end{aligned} \quad (57)$$

The first term in the r.h.s. of Eq. (57) describes the voltage bias between the reservoirs of  $\varphi$  and  $\psi$ -particles, while the second term has an appearance of the  $k$ -conserving ‘‘tunneling’’ with  $V$ -dependent ‘‘tunneling amplitude’’. These two contributions correspond to the two terms in the r.h.s. of Eq. (42). Similarly, the current operator  $j$ , see Eq. (39), can be also split into two contributions:

$$\begin{aligned} j &= j_0 + \delta j, \\ j_0 &= \frac{i}{2} [H_{eff} + H_V, \hat{N}_\psi - \hat{N}_\varphi] = ieV\theta_0 \sum_{ks} \varphi_{ks}^\dagger \psi_{ks} + \text{H.c.}, \\ \delta j &= -\theta_0 \frac{d}{dt} \hat{A}. \end{aligned} \quad (58)$$

It turns out that  $\delta j$  in Eq. (58) makes no contribution to the average current in the leading (second) order in  $\theta_0$ . Indeed, in this order

$$\langle \delta j \rangle = i\theta_0^2 eV \frac{d}{dt} \int_{-\infty}^t dt' \langle [\hat{A}(t), \hat{A}(t')] \rangle_0,$$

where  $\langle \dots \rangle_0$  denotes thermodynamic averaging with the Hamiltonian  $H_0 = H_{eff} + H_V(0)$ . The thermodynamic (equilibrium) averaging is well defined here because the ‘‘tunneling’’ term in Eq. (57) is absent at  $\theta_0 = 0$ . Taking into account that  $\langle [\hat{A}(t'), \hat{A}(t)] \rangle_0$  depends only on  $t - t' = \tau$ , we find

$$\langle \delta j \rangle = i\theta_0^2 eV \frac{d}{dt} \int_0^\infty d\tau \langle [\hat{A}(\tau), \hat{A}(0)] \rangle_0 \equiv 0.$$

To the contrary, the term  $j_0$  in Eq. (58) makes a finite contribution to the average current. Evaluation of this contribution in the leading order in  $\theta_0$  proceeds similarly to the calculation of the tunneling current between two massive conductors (see, e.g., [31]), and yields for the differential conductance across the dot

$$dI/dV = G_0 \int d\omega (-df/d\omega) \frac{1}{2} \sum_s [-\pi\nu \text{Im} T_s(\omega + eV)] \quad (59)$$

with

$$G_0 = \frac{2e^2}{h} (2\theta_0)^2 \approx \frac{8e^2}{h} \left| \frac{t_{L0}}{t_{R0}} \right|^2.$$

Note that the  $V \rightarrow 0$  limit of Eq. (59) coincides with the small  $\theta_0$  limit of the linear response result Eq. (43). Using now Eqs. (46),(47),(55), and (59) we obtain for the differential conductance at  $T \ll eV \ll \delta E$

$$\frac{dI}{dV} = \begin{cases} G_0 \left[ 1 - \frac{3}{2} \left( \frac{eV}{T_K} \right)^2 \right], & eV \ll T_K \\ G_0 \frac{3\pi^2/16}{[\ln(eV/T_K)]^2}, & eV \gg T_K \end{cases} \quad (60)$$

Thus, a large voltage bias  $eV \gg T$  has qualitatively the same destructive effect on the Kondo physics as the temperature does. If temperature  $T$  exceeds the bias,  $T \gg eV$ , the differential conductance  $dI/dV$  coincides with the linear conductance  $G$ , see Eqs. (48),(56) above.

## 6. Conclusion

In the simplest form of the Kondo effect considered in this article, a quantum dot behaves essentially as a magnetic impurity with spin 1/2 coupled via exchange interaction to two conducting leads [24]. However, the characteristic energy scale for the intra-dot excitations is much smaller than the corresponding scale for a real magnetic impurity. This allows one to induce some degeneracies in the ground state of a dot which are more exotic than just the spin degeneracy considered above. One of the possibilities is to create a degeneracy between a singlet state and a component of a triplet state by applying a magnetic field to a dot with an even number of electrons. Depending on the relation between the Zeeman energy and the value of the diamagnetic shift of orbital levels in a magnetic field, this degeneracy gives rise to various ‘‘flavors’’ of the Kondo effect. A review of the corresponding experiments and theory can be found in [37]

In our discussion of the Kondo effect we assumed that the dot remains close to an equilibrium state even under the conditions of an electron transport experiment. In fact, this limitation led us to consider a very asymmetric setup of a quantum dot device in Sec. 5.2, where the non-linear electron transport is discussed. One of the advantages of quantum dots, however, is that these devices allow one to study the Kondo effect in truly out-of-equilibrium conditions. Such conditions may be created by applying a significant dc bias between the leads, or by irradiating a dot by microwaves [38]. In the latter case one can monitor the ‘‘health’’ of the Kondo effect by measuring the linear dc conductance at the same time. It turns out that microwaves suppress the effect [38] by destroying the coherence of the spin state of the dot [39]. In the former case, one can apply a strong magnetic field in addition to biasing the dot. Zeeman splitting then leads to peaks in the differential conductance at a finite bias [40, 41]. Interest to this problem was recently revived, see, e.g., [42] and references therein.

These are only a few out of many possible extensions of the simple model discussed in this review.

### Acknowledgements

This work is supported by NSF grants DMR97-31756, DMR02-37296, and EIA02-10736.

### References

1. L.P. Kouwenhoven *et al.*, in *Mesoscopic Electron Transport*, eds. L.L. Sohn, L.P. Kouwenhoven, and G. Schön (Kluwer, Netherlands, 1997), p. 105.
2. P. Joyez *et al.*, *Phys. Rev. Lett.* **79**, 1349 (1997).
3. D. Goldhaber-Gordon *et al.*, *Nature* (London) **391**, 156 (1998); S.M. Cronenwett, T.H. Oosterkamp, and L.P. Kouwenhoven, *Science* **281**, 540 (1998); J. Schmid *et al.*, *Physica* (Amsterdam) **256B-258B**, 182 (1998). *Science* **289**, 2105-2108 (2000).
4. L. Kouwenhoven and L. Glazman, *Physics World* **14**, 33 (2001).
5. J. Kondo, *Prog. Theor. Phys.* **32**, 37 (1964).
6. C.W.J. Beenakker, *Rev. Mod. Phys.* **69**, 731 (1997).
7. M.L. Mehta, *Random Matrices* (Academic Press, New York, 1991).
8. B.L. Altshuler *et al.*, *Phys. Rev. Lett.* **78**, 2803 (1997); O. Agam *et al.*, *Phys. Rev. Lett.* **78**, 1956 (1997); Ya.M. Blanter, *Phys. Rev. B* **54**, 12807 (1996); Ya.M. Blanter and A.D. Mirlin, *Phys. Rev. E* **55**, 6514 (1997); I.L. Aleiner and L.I. Glazman, *Phys. Rev. B* **57**, 9608 (1998).
9. I.L. Aleiner, P.W. Brouwer, and L.I. Glazman, *Phys. Rep.* **358**, 309 (2002).
10. J. Davidovic and M. Tinkham, *Phys. Rev. Lett.* **83**, 1644 (1999).
11. M.P.A. Fisher and L.I. Glazman, in *Mesoscopic Electron Transport*, eds. L.L. Sohn, L.P. Kouwenhoven, and G. Schön (Kluwer, Netherlands, 1997), p. 331.
12. J.M. Ziman, *Principles of the Theory of Solids*, (Cambridge University Press, Cambridge, 1972), p.339.
13. P.W. Brouwer, Y. Oreg, and B.I. Halperin, *Phys. Rev. B* **60**, R13 977 (1999); H.U. Baranger, D. Ullmo, and L.I. Glazman, *Phys. Rev. B* **61**, R2425 (2000); I.L. Kurland, I.L. Aleiner, and B.L. Altshuler, *Phys. Rev. B* **62**, 14886 (2000).
14. Y. Alhassid, *Rev. Mod. Phys.* **72**, 895 (2000).
15. I.O. Kulik and R.I. Shekhter, *Sov. Phys. JETP* **41**, 308 (1975); L.I. Glazman and R.I. Shekhter, *J. Phys. Cond. Matt.* **1**, 5811 (1989).
16. I. Giaever and H.R. Zeller, *Phys. Rev. Lett.* **20**, 1504 (1968); H.R. Zeller and I. Giaever, *Phys. Rev.* **181**, 789 (1969).
17. D.V. Averin and Yu.V. Nazarov, *Phys. Rev. Lett.* **65**, 2446 (1990).
18. A.A. Abrikosov, *Fundamentals of the Theory of Metals*, (North-Holland, Amsterdam, 1988), p. 620.
19. I.L. Aleiner and L.I. Glazman, *Phys. Rev. Lett.* **77**, 2057 (1996).
20. L.I. Glazman and M.E. Raikh, *JETP Lett.* **47**, 452 (1988); T.K. Ng and P.A. Lee, *Phys. Rev. Lett.* **61**, 1768 (1988).
21. W.G. van der Wiel *et al.*, *Phys. Rev. Lett.* **88**, 126803 (2002).
22. C. B. Duke, *Tunneling in Solids* (Academic Press, New York, 1969); J. M. Rowell, in *Tunneling Phenomena in Solids*, eds. E. Burstein and S. Lundqvist (Plenum, New York, 1969), p. 385.

23. A.F.G. Wyatt, Phys. Rev. Lett. **13**, 401 (1964); R.A. Logan and J.M. Rowell, Phys. Rev. Lett. **13**, 404 (1964).
24. J. Appelbaum, Phys. Rev. Lett. **17**, 91 (1966); P.W. Anderson, Phys. Rev. Lett. **17**, 95 (1966).
25. M. Pustilnik and L.I. Glazman, Phys. Rev. Lett. **87**, 216601 (2001).
26. A.M. Tsvelick and P.B. Wiegmann, Advances in Phys. **32**, 453 (1983); N. Andrei, K. Furuya, and J.H. Lowenstein, Rev. Mod. Phys. **55**, 331 (1983).
27. M. Pustilnik and L.I. Glazman, Phys. Rev. B **64**, 045328 (2001).
28. P.W. Anderson, *Basic Notions of Condensed Matter Physics* (Addison-Wesley, Reading, 1997).
29. K.G. Wilson, Rev. Mod. Phys. **47**, 773 (1975).
30. L.I. Glazman, F.W.J. Hekking, and A.I. Larkin, Phys. Rev. Lett. **83**, 1830 (1999).
31. G.D. Mahan, *Many-Particle Physics* (Plenum, New York, 1990).
32. P.W. Anderson, J. Phys. C **3**, 2436 (1970).
33. A.A. Abrikosov, Physics **2**, 21 (1965).
34. P. Nozières, J. Low Temp. Phys. **17**, 31 (1974); J. Physique **39**, 1117 (1978).
35. I. Affleck and A.W.W. Ludwig, Phys. Rev. B **48**, 7297 (1993).
36. T.A. Costi, A.C. Hewson, and V. Zlatić, J. Phys.: Cond. Mat. **6**, 2519 (1994).
37. M. Pustilnik *et al.*, Lecture Notes in Physics, **579**, 3 (2001).
38. J.M. Elzerman *et al.*, J. Low Temp. Phys. **118**, 375 (2000).
39. A. Kaminski, Yu.V. Nazarov, and L.I. Glazman, Phys. Rev. Lett. **83**, 384 (1999).
40. J.A. Appelbaum, Phys. Rev. **154**, 633 (1967).
41. Y. Meir, N.S. Wingreen, and P.A. Lee, Phys. Rev. Lett. **70**, 2601 (1993).
42. A. Rosch *et al.*, Phys. Rev. Lett. **90**, 076804 (2003).